In adlayers on *c*-plane InN surfaces: A polarity-dependent study by x-ray photoemission spectroscopy

T. D. Veal,* P. D. C. King, P. H. Jefferson, L. F. J. Piper, and C. F. McConville
Department of Physics, University of Warwick, Coventry CV4 7AL, United Kingdom

Hai Lu† and W. J. Schaff
Department of Electrical and Computer Engineering, Cornell University, Ithaca, New York 14853, USA

P. A. Anderson and S. M. Durbin
Department of Electrical and Computer Engineering, MacDiarmid Institute for Advanced Materials and Nanotechnology, University of Canterbury, Christchurch 8140, New Zealand

D. Muto, H. Naoi, and Y. Nanishi
Department of Photonics, Ritsumeikan University, 1-1-1 Noji-Higashi, Kusatsu, Shiga 525-8577, Japan
(Received 30 April 2007; published 9 August 2007)

The surfaces of In- and N-polarity InN grown by molecular-beam epitaxy have been investigated using core-level and valence band x-ray photoemission spectroscopy (XPS). From the ratio of the In and N core-level XPS signal intensities, the clean InN surfaces have been found to be terminated by In adlayers, in agreement with the predictions of previous first-principles calculations. The In- and N-polarity surfaces are terminated by ~3.4 and ~2.0 ML of In, in each case 1 ML more than for Ga on GaN surfaces under metal-rich growth conditions. The valence band XPS indicates a valence band maximum to surface Fermi level separation of 1.32 ± 0.10 eV for both In- and N-polarity InN surfaces, indicating that the surface space charge is independent of polarity and, unlike for GaN, is not significantly affected by spontaneous polarization. This is due to the In coverage on the surface of InN of both polarities being sufficient to efficiently screen the polarization charge.

DOI: 10.1103/PhysRevB.76.075313 PACS number(s): 68.35.Bs, 68.47.Fg, 79.60.−i, 73.61.Ey

I. INTRODUCTION

Extreme electron accumulation at the surface of InN has been the subject of several recent experimental studies using a variety of different techniques.[1–4] The origin of the electron accumulation has been explained in terms of the conduction band minimum at the Γ-point lying below the charge neutrality level or branch point energy.[5] This allows donor-type surface states to be unoccupied and positively charged, contributing their electrons into the accumulation layer and causing downward band bending. Despite this explanation of the overriding band structure property responsible for the electron accumulation, a microscopic origin of the phenomenon has only very recently been proposed. Based on first-principles calculations, it has been suggested that the donor-type surface states are associated with In-In bonds in a surface In adlayer.[6]

The influence of the InN film polarity, surface reconstruction, and surface stoichiometry on the electron accumulation has yet to be investigated experimentally. This is in contrast to GaN, where the Fermi level at the surface of N-polarity GaN has been found to be up to 1.4 eV higher than that at the Ga-polarity surface.[7] Additionally, while relatively little attention has been paid to the chemical and the structural nature of InN surfaces, extensive studies of the GaN surface structure have revealed a strong tendency for Ga atoms to stabilize in the surface layer. This is the dominant force driving GaN surface reconstruction, overriding the usual principal mechanisms for conventional III-V semiconductors of obeying electron counting and reducing the number of dangling bonds. Consequently, GaN grown under Ga-rich conditions has surface reconstructions involving Ga adlayers, the coverage of which has been found to depend on the polarity of the GaN, with 1.1 ML of Ga on GaN$(000\bar{1})$ and 2.4 ML on GaN(0001),[8] in agreement with the predictions of first-principles theory.[9,10]

The propensity for GaN surfaces to be stabilized by Ga adlayers is due to the small lattice constant and high anion-anion bond strength compared to those of conventional III-V semiconductors.[11] The expectation from theoretical studies has long been that all polar III-nitride surfaces (including those of InN) will resemble those of GaN.[11] This idea that group III atom stabilization of the surface is a general property of III-nitrides is supported by evidence of Al adlayers on AlN(0001) surfaces[12] and In adlayers on InGaN(0001) surfaces.[13]

Recently, first-principles calculations have shown that In adlayers at *c*-plane InN surfaces are energetically favorable.[6,14] Moreover, the existence of In adlayers at InN(0001) and $(000\bar{1})$ surfaces has been tentatively inferred from both core-level x-ray photoelectron spectroscopy of the surface In:N ratio[15] and growth studies of InN.[16–18] Meanwhile, in our previous work, we speculated that differences between experimental valence band spectra and the calculated bulk valence band density of states were due to surface-related effects.[19] These recent studies of InN and the previous GaN results have prompted the present investigation of the polarity dependence of the surface stoichiometry and surface Fermi level position of InN using core-level and valence band photoemission spectroscopies.

 ©2007 The American Physical Society

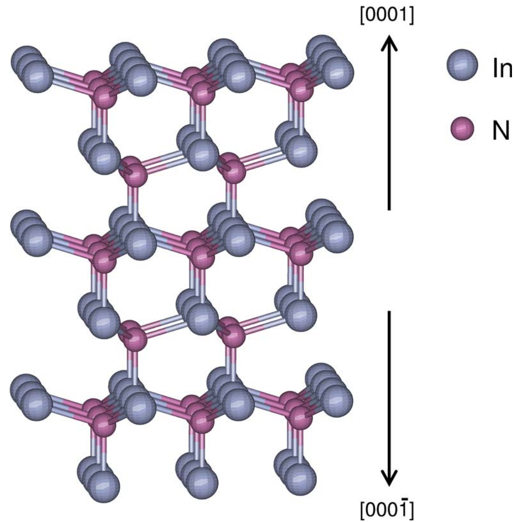

FIG. 1. (Color online) Ball and stick model illustrating the In-polarity $[0001]$ and N-polarity $[000\bar{1}]$ directions of wurtzite InN. The surfaces of the In- and N-polarity faces of InN are both shown with In termination.

The property of polarity in InN and wurtzite III-nitrides, in general, is due to their reduced symmetry compared with conventional zinc-blende III-V semiconductors. Although the atoms are tetrahedrally bonded in both structures, unlike zinc-blende crystals, where the $[001]$ and $[00\bar{1}]$ crystallographic directions are equivalent, in wurtzite crystals, the $[0001]$ and $[000\bar{1}]$ directions are different, as shown in Fig. 1. In the wurtzite structure, the In polarity (N polarity) is defined as the orientation of the crystal such that only a single bond from the In (N) is directed toward the surface along the c axis.[20] The In (N) atom is also bonded to three N (In) atoms in the direction away from the surface. The upper surface of the model in Fig. 1 is the bulk-like In termination of the In-polarity crystallographic direction, $[0001]$, while the lower surface is the bulk-like In termination of the N-polarity crystallographic direction, $[000\bar{1}]$. The bulk-like

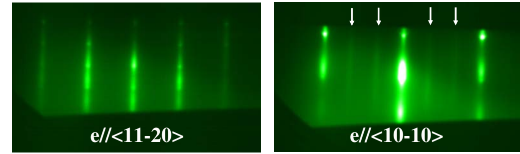

FIG. 2. (Color online) (1×3) RHEED pattern observed from an In-polarity sample (R963) indicating a $(\sqrt{3}\times\sqrt{3})R30°$ reconstruction.

N termination of each polarity is obtained by removing the surface layer of In atoms.

II. EXPERIMENTAL DETAILS

The InN samples used in this study were grown by molecular-beam epitaxy (MBE) at Ritsumeikan, Canterbury, and Cornell Universities. Details of the substrate, nitridation temperature, buffer layers, growth temperatures, InN film thickness and resulting polarity, average electron density, and mobility of the InN film are presented for each sample in Table I. After the growth of InN at Ritsumeikan, reflection high-energy electron diffraction (RHEED) was used to characterize the surface structure of the InN films. The N-polarity and mixed polarity samples exhibited (1×1) RHEED patterns. The RHEED patterns from an In-polarity sample are shown in Fig. 2 and indicate a $(\sqrt{3}\times\sqrt{3})R30°$ reconstruction. A piece of each InN film was etched by a 10 mol/1 KOH solution for 60 min at room temperature. The surface morphology of the samples before and after etching was examined by scanning electron microscopy (SEM) in order to infer the polarity. The efficacy of using wet etching and SEM to determine the polarity of InN samples has previously been confirmed by convergent beam electron diffraction.[21]

The x-ray photoemission spectroscopy (XPS) analysis was performed using a Scienta ESCA300 spectrometer at the National Centre for Electron Spectroscopy and Surface analysis, Daresbury Laboratory, UK. This consists of a rotating anode Al $K\alpha$ x-ray source ($h\nu$=1486.6 eV), x-ray mono-

TABLE I. Details of the InN samples used in this study. Sample code letters "R," "C," and "GS" correspond to samples grown at Ritsumeikan, Canterbury, and Cornell Universities, respectively. The temperatures given are those measured in the respective MBE chambers. No calibration has been performed to put them on an absolute scale.

Sample	R963	C217	GS1469	R971	R941	C283
Polarity	In	In	In	Mixed[a]	N	N
Substrate	Al_2O_3	YSZ	Al_2O_3	Al_2O_3	Al_2O_3	Al_2O_3
Nitridation temp. (°C)	550	None	200	550	550	650
Buffer layer	GaN	None	GaN/AlN	GaN	InN	GaN
Buffer growth temp. (°C)	300	None	750/800	300	300	650
InN film thickness (nm)	230	500	350	230	500	500
InN growth temp. (°C)	450	400	480	450	550	450
n (10^{18} cm^{-3})	20	2.4	1.9	8.1	6.7	23
μ (cm^2 V^{-1} s^{-1})	116	125	1030	532	566	71

[a]From SEM analysis after KOH etching, this sample is estimated to be 55(±5%) In polar and 45(±5%) N polar.

chromator, and 300 mm mean radius spherical-sector electron energy analyzer with parallel electron detection system. The analyzer was operated with 0.8 mm slits and at a pass energy of 150 eV. Gaussian convolution of the analyzer broadening with an effective linewidth of 0.27 eV for the x-ray source gives an effective instrument resolution of 0.45 eV. The Fermi level position (zero of the binding energy scale) was calibrated using the Fermi edge of an ion bombarded silver reference sample, which is regularly used to calibrate the spectrometer.

Following insertion into the XPS vacuum chamber, both core-level and valence band spectra were recorded from the "untreated" InN samples. After these initial XPS measurements, InN surface preparation was achieved *in situ* by atomic hydrogen cleaning (AHC). The AHC process typically consisted of a 20 kL dose of molecular hydrogen being passed through a thermal gas cracker with a cracking efficiency of ~50% while annealing the sample at a temperature of 275 °C. This temperature is significantly below the growth temperature. After AHC, XPS spectra were recorded at room temperature from the "cleaned" InN samples. Because excessive exposure to atomic hydrogen is known to etch InN and produce indium droplets,[19] particularly on the N-polarity InN surface,[22] all samples were analyzed by SEM and atomic force microscopy after the XPS measurements. Only XPS results from samples where no indium droplets were produced are presented.

Ideally, the photoemission analysis of the polarity dependence of the surface Fermi level and surface stoichiometry would be performed in the MBE growth chamber or in an attached vacuum chamber. However, for other III-V semiconductors, exposure of the surface to atmosphere followed by cleaning in the analysis chamber produces the same cation-rich reconstructions obtained by MBE, such as the (4×2) reconstructions on InAs(001) and InSb(001), (1×3) on GaSb(001), and (2×2) on InAs(111)A.[23] Therefore, photoemission spectroscopy of the various InN films has been performed both after exposure of the surface to atmosphere and after cleaning the surface with atomic hydrogen.

III. RESULTS, ANALYSIS, AND DISCUSSION

A. Valence band spectra of untreated InN surfaces

The valence band XPS spectra recorded from a range of different c-plane InN thin films before any surface cleaning are shown in Fig. 3. The intensity ratio of the two valence band peaks varies as a function of the polarity. For the In-polarity films, the 3 eV valence band peak is more intense than the 6.5 eV peak, while the reverse is true for the N-polarity films. An additional mixed polarity InN film grown under unoptimized conditions, which is estimated from SEM of a KOH-etched part of the sample to be 55% In polarity and 45% N polarity, was also analyzed. Its valence band peak intensities lie between those of the In- and N-polarity samples. The three spectra from the three different In-polar InN samples (MBE grown in three different laboratories by different methods) are the same. Similarly, the two spectra from the two different N-polarity InN samples are also very similar. This indicates that the valence band spectrum is characteristic of the InN film polarity and reflects the polarity dependence of the surface termination and the contribution to the valence band spectrum of the associated surface valence band density of states. The coincidence of the leading edge of the valence band also gives the first indication that the valence band maximum (VBM) to surface Fermi level separation is independent of the polarity.

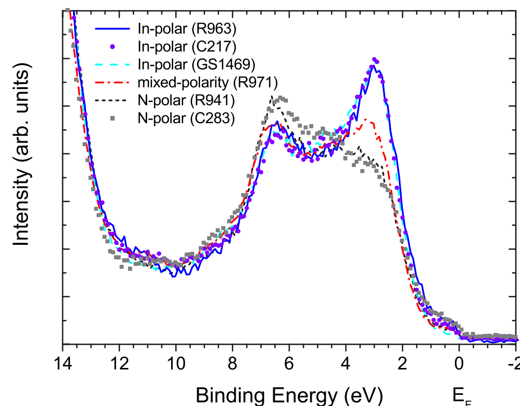

FIG. 3. (Color online) Valence band XPS spectra recorded using a photoelectron emission angle of 90° from InN films of different polarities grown at Ritsumeikan (solid, dashed-dotted, and short dashed lines), Canterbury (dark and light points) and Cornell (dashed line). The data were recorded before any surface preparation was performed. The intensity scale of each spectrum has been normalized so that all spectra have a common background intensity in the 9–12 eV region. The zero of the binding energy scale corresponds to the Fermi level E_F.

B. Atomic hydrogen cleaning of InN

In order to further investigate both this aspect of the valence band spectra and the polarity dependence of the surface stoichiometry without the influence of effects due to the native oxide, the InN samples were cleaned using atomic hydrogen. The In $3d$, N $1s$, and O $1s$ core-level XPS spectra recorded from an In-polarity InN sample before and after cleaning are shown in Fig. 4. The In $3d_{5/2}$ and In $3d_{3/2}$ peaks before cleaning consist of In-N components at 444.0 and

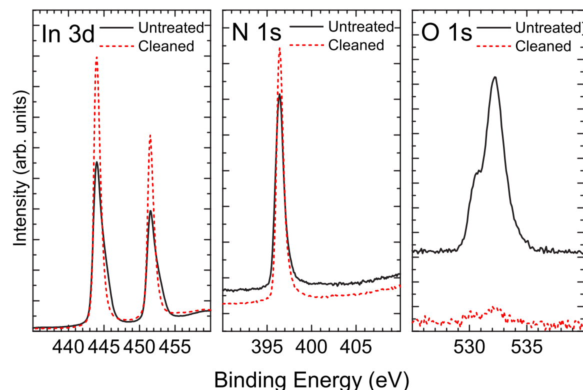

FIG. 4. (Color online) In $3d$, N $1s$, and O $1s$ core-level spectra recorded using an emission angle of 90° from an untreated (solid lines) and a cleaned (dashed lines) In-polarity InN film.

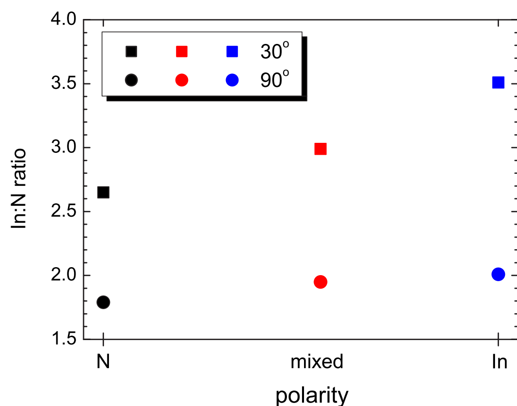

FIG. 5. (Color online) XPS In:N intensity ratios for In-polarity, mixed polarity, and N-polarity InN samples recorded at emission angles of 90° (circles) and 30° (squares) with respect to the surface plane.

451.6 eV, respectively, and each has a higher binding energy shoulder due to In-O components. After cleaning, the high binding energy components are absent and an In-N bonding component remains, indicating the removal of the oxygen bonded to indium. The N 1*s* peak at 396.4 eV is due to N-In bonding, with no contamination-related components present either before or after cleaning. Before cleaning, the O 1*s* peak consists of a component at 532.2 eV due to adventitious oxygen (physisorbed rather than chemisorbed) and a lower intensity component at 530.6 eV due to In-O bonding. The oxide coverage before cleaning is estimated to have been between 15 and 25 Å. After accounting for the atomic sensitivity factors, the contribution of the oxygen to the total XPS signal changes from 26% before cleaning to less than 1% after cleaning. The core-level spectra from the mixed polarity sample and N-polarity samples indicated similar reduction in oxygen coverage as a result of cleaning.

C. Core-level intensity ratios of cleaned InN surfaces

The In:N XPS intensity ratio, calculated from the core-level peak areas divided by the atomic sensitivity factors for each core level for the Scienta ESCA300 spectrometer, is shown in Fig. 5 as a function of polarity for two different emission angles. The In:N ratio is greater in each case for the more surface sensitive 30° emission than for the 90° emission and the In:N ratio also increases on going from N polarity to In polarity. These results indicate that all the samples have In-rich surfaces and that the surface of the In-polarity InN is more In rich than the surface of the N-polarity InN.

To obtain quantitative values of the In coverage on the different samples from the XPS core-level results, the In:N intensity ratios have been compared with model calculations for the different surface reconstructions of In- and N-polarity InN shown in Figs. 6(a)–6(f) and Figs. 6(g)–6(k), respectively. The reconstructions are shown in order of increasing In coverage. For In-polarity InN, the first three consist of N-terminated bulk [Fig. 6(a)], In-terminated bulk [Fig. 6(b)], and In-terminated bulk plus a laterally contracted indium monolayer, containing 4/3 of the indium of a bulk-like layer [Fig. 6(c)]. The subsequent In-polarity InN surface reconstructions shown are all terminated with this laterally contracted layer but have one to three additional bulk-like In layers immediately below [Figs. 6(d)–6(f)]. The N- and In-terminated bulk cases are included as the most "naive" reconstructions to be eliminated. The use of the laterally contracted In-terminated reconstructions is based on the observation by RHEED of a $(\sqrt{3}\times\sqrt{3})R30°$ reconstruction after the growth of In-polarity InN (Fig. 2), the theoretically predicted and experimentally observed laterally contracted Ga bilayers on Ga-polarity GaN surfaces,[9] and the results of recent first-principles calculations of the energies of InN(0001) surface reconstructions.[14]

While the laterally contracted Ga bilayer on GaN(0001) is generally found to be incommensurate, being described as a "pseudo-(1×1)-structure" from electron diffraction data, for computational convenience, it has been modeled using a $(\sqrt{3}\times\sqrt{3})$ cell.[9] However, a $(\sqrt{3}\times\sqrt{3})R30°$ reconstruction on a GaN(0001) surface has recently been observed by low-energy electron diffraction.[24] The laterally contracted Ga bilayer was found to be energetically favorable due to the reduced Ga-Ga spacing with respect to that of the bulk. The stability of the reconstruction was found to be insensitive to the registry of the contracted layer relative to the substrate.[9,25] The top view of a $(\sqrt{3}\times\sqrt{3})R30°$ laterally contracted overlayer in InN is shown in Fig. 7. Both the RHEED and XPS In:N intensity ratio are insensitive to the registry of the overlayer with respect to the bulk; the RHEED is sensitive only to the lateral periodicity and the XPS In:N ratio to the composition of the layers along the growth direction. In a $(\sqrt{3}\times\sqrt{3})$ unit cell, there are four atoms in the laterally contracted hexagonal overlayer for every three atoms in the underlying hexagonal layers, resulting in the overlayer containing 4/3 ML of indium.

For N-polarity InN, the reconstructions, shown in order of increasing In coverage, are N terminated [Fig. 6(g)], In terminated [Fig. 6(h)], and In terminated with between one and three additional In adlayers [Figs. 6(i)–6(k)]. For the N-polarity case, the topmost layer has no lateral contraction, in accordance with the results of our InN RHEED measurements and the first-principles calculations of surface reconstructions of both GaN and InN.[10,14]

The XPS In:N ratios calculated for 90° and 30° emission angles from the different surface reconstructions are shown in Fig. 8 for In- and N-polarity InN. The calculations of the core-level photoemission intensity ratios use a layer-attenuation model based on photoelectron inelastic mean free paths (IMFPs) calculated using the TPP-2M predictive formula of Tanuma *et al.*[26] The calculated intensity ratios are not sensitive to small variations in either these IMFPs or the spacings between layers. However, the intensity ratios vary significantly with both the number of surface indium layers and the concentration of indium within the layers.

The experimental XPS In:N ratios are also indicated in Fig. 8 for In- and N-polarity InN. Comparison of the model calculations with the measured XPS In:N ratios indicates that the In-polarity InN has ~3.4 ML of In above the In-terminated InN bulk [Fig. 6(e)] and the N-polarity InN has

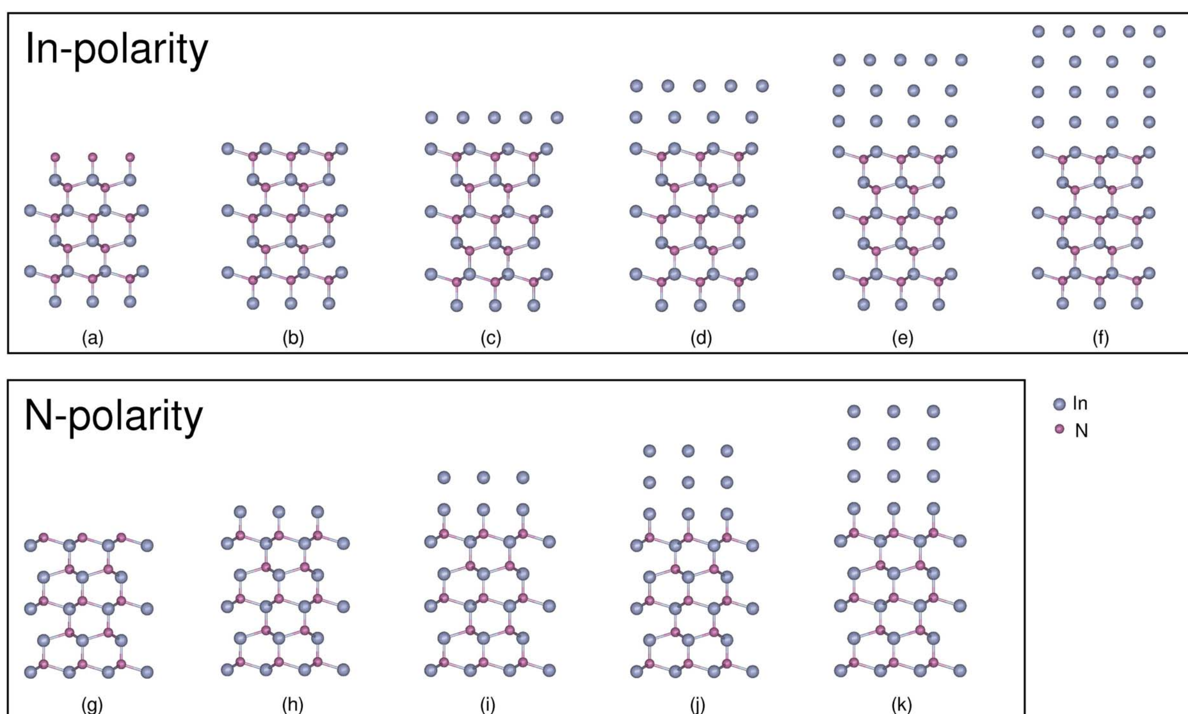

FIG. 6. (Color online) Ball and stick representations of the different surface reconstructions used to model the In:N XPS ratios. (a)–(f) are In-polarity InN, where the reconstructions are as follows (with In coverages in monolayers with respect to the In-terminated bulk to correspond to Fig. 8 in parentheses): (a) N terminated (−1), (b) In terminated (0), (c) a laterally contracted In monolayer (1.33), (d) an In bilayer with laterally contracted top layer (2.33), (e) an In trilayer with laterally contracted top layer (3.33), and (f) an In quadlayer with laterally contracted top layer (4.33). In each case, the laterally contracted top layer contains 4/3 of a monolayer of indium, as illustrated in Fig. 7. In this projection, the laterally contracted layer is shown rotated by 30° into the plane of the other layers for ease of viewing. (g)–(k) are N-polarity InN, where the reconstructions are (g) N terminated (−1), (h) In terminated (0), (i) an In monolayer (1), (j) an In bilayer (2), and (k) an In trilayer (3).

~2.0 ML of In above the In-terminated InN bulk [Fig. 6(j)]. These In coverages are both 1 ML greater than the Ga coverages for the respective GaN surfaces grown under Ga-rich conditions. Additionally, these In coverages are greater than the highest coverages for which theoretical calculations have been performed for wurtzite InN.[14] However, for InN(111), which is very similar to InN(0001) in total-energy terms, 3 ML of In on top of In-terminated InN(111) has been found to be more energetically favorable than lower InN coverages.[27] The theoretical studies of both the polar wurtzite InN surfaces and InN(111) indicate that there is a stronger tendency for metallic overlayers to form on InN than on GaN.

Two properties unique to group-III nitrides are responsible for the unusual stability of group-III-rich reconstructions previously observed on GaN surfaces, compared with that on conventional III-V surfaces. Firstly, Ga atoms on GaN form stronger Ga-Ga bonds than on, for example, GaAs. The origin of the stronger bonding lies in the sizable mismatch of the covalent radii of Ga and N. Because of the small radius of the N atoms, the Ga atoms in GaN have approximately the same distance between them as in bulk Ga. The Ga atoms on the surface can form metallic bonds similar to those in Ga metal even without any relaxation, thus stabilizing the Ga-terminated surface.[28] As there is an even greater mismatch between the covalent radii of In and N than for Ga and N, the In-In bonds are expected to be

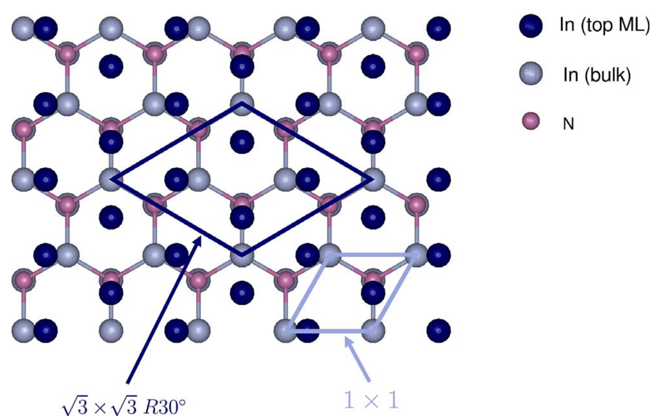

FIG. 7. (Color online) A schematic top view showing a laterally contracted hexagonal overlayer of In atoms (dark large circles) above a hexagonal substrate layer (consisting of large light circles for In atoms and small circles for N atoms). The lattice vectors of the overlayer are rotated by 30° with respect to those of the substrate. A representative $(\sqrt{3}\times\sqrt{3})R30°$ unit cell of the laterally contracted layer and a (1×1) unit cell of the unreconstructed second layer are shown. In these $(\sqrt{3}\times\sqrt{3})$ unit cells, there are four atoms in the laterally contracted hexagonal overlayer for every three atoms in the underlying hexagonal layers.

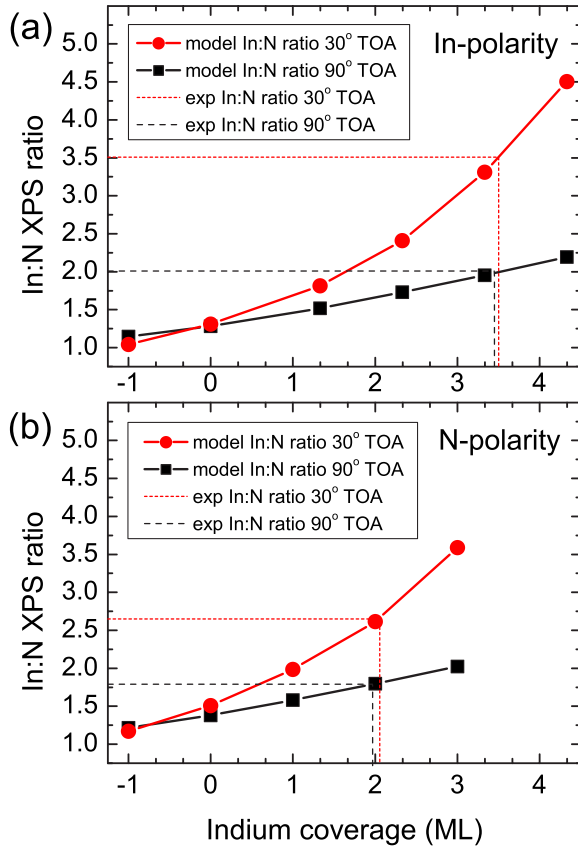

FIG. 8. (Color online) XPS In:N intensity ratios for 90° (squares) and 30° (circles) take-off angles (TOA) or emission angles (with respect to the surface plane) calculated for the surface of (a) In-polarity InN(0001) and (b) N-polarity InN(000$\bar{1}$) for different surface indium coverages in monolayers with respect to the In-terminated bulk, as detailed in Fig. 6. The fractional monolayer coverages correspond to the topmost layer being laterally contracted with 4/3 of the indium atoms of a bulk-like indium layer. The solid lines between the calculated points are guides to the eyes. The experimentally determined XPS In:N intensity ratios for 90° and 30° emission angles are indicated by long and short dashed lines, respectively.

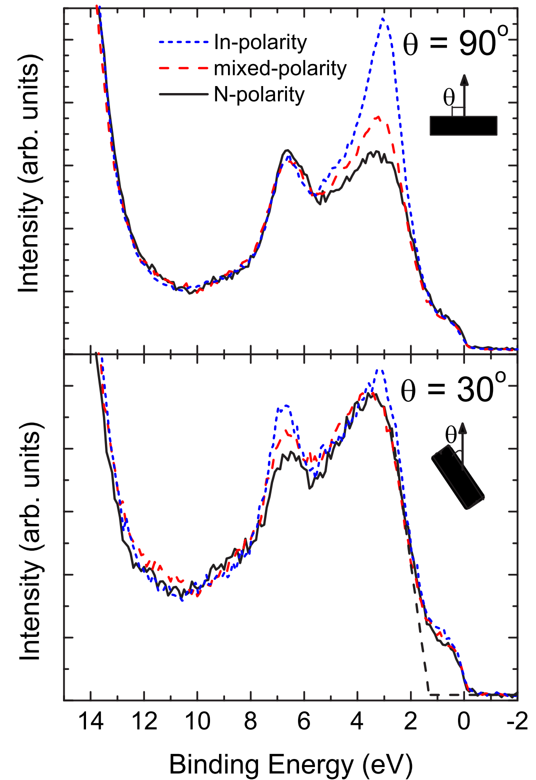

FIG. 9. (Color online) The valence band spectra from In-polarity, mixed polarity, and N-polarity InN samples after atomic hydrogen cleaning, recorded using emission angles of 90° and 30° with respect to the surface plane. The extrapolation of the leading edge of the valence band emission to the base line indicates that the VBM to surface Fermi level separation is 1.32±0.10 eV for all three samples.

strong on InN, enabling the stabilization of In-terminated surfaces.

The second mechanism stabilizing metal surfaces on group-III nitrides is the very different cohesive energies of the bulk phases of the group-III metal and N. The cohesive energy of bulk Ga is 2.81 eV/atom while that of the N_2 molecule is 5.0 eV/atom. In contrast, the cohesive energy of bulk As (2.96 eV/atom) is only slightly larger than that of bulk Ga. Because of this asymmetry between the Ga and N "reservoirs," more energy is needed to transfer N atoms from its reservoir to the surface than to transfer Ga atoms to the surface.[28] Moreover, because the cohesive energy of bulk In is 2.5 eV/atom[29] (even further from that of the N_2 molecule than bulk Ga), stabilization of a group-III-terminated surface may be even more favorable for InN than for GaN.

The different In coverages observed on In-polar InN (~3.4 ML) and N-polar InN (~2.0 ML) may be responsible for the different growth behaviors of InN of opposite polarity. For N-polar InN epitaxy, a step height of up to 2–4 ML is typically seen for the smoothest surface, whereas for In-polar InN epitaxy, a 1 ML stepped flat surface can be obtained.[18] The behaviors of excess In on the growth front are different for the two polarities. During growth of N-polar InN, In droplets have a tendency to form on the growing surface under all but the most optimized conditions, disturbing the growth and roughening the surface. However, this is not the case for In-polar InN epitaxy, when In-rich conditions are employed. Any excess In can migrate more easily on the In-polar surface than on the N-polar surface, leaving most of the surface free of droplets and covered by multiple layers of In. This is believed to be very helpful for the continuous growth of InN in an In-rich regime.[18]

D. Valence band spectra of cleaned InN surfaces

The valence band XPS spectra recorded at emission angles of 90° and 30° with respect to the surface plane from different polarity InN thin films after surface cleaning are shown in Fig. 9. For the 90° emission spectra, the intensity ratio of the two valence band peaks varies as a function of the polarity in the same way as before cleaning, with the 3 eV valence band peak reducing in relative intensity on going from In to N polarity. However, for the 30° emission

spectra, it is the 6.5 eV valence band peak that reduces in relative intensity on going from In to N polarity. Since the 30° emission spectra probe half the depth of the 90° emission spectra, these differences reflect the difference between the surface and bulk valence band densities of states (VBDOS); the spectra recorded at the two emission angles both contain contributions from the surface and bulk VBDOS. A larger proportion of the 30° emission XPS signal, compared to the case of the 90° emission, is from the surface VBDOS. To obtain information about the polarity dependence of the surface structure of InN, these valence band spectra must be compared with the surface VBDOS calculated from first principles for different polarities and surface reconstructions. The results of such calculations are not yet available.

However, in spite of the difficulties associated with interpreting the 3 and 6.5 eV valence band peaks, the close to Fermi level emission provides another qualitative indication that the In coverage is greater on the surface of the In-polarity InN than for the N polarity. The emission close to the Fermi level is associated with the metallic In adlayers on the surface. A similar feature in XPS spectra from GaN(0001) surfaces has previously been attributed to the presence of Ga adlayers.[30] In the most surface sensitive data (30° emission, Fig. 9), the intensity of the feature increases on going from N to In polarity, consistent with the increasing surface In coverage indicated by the core-level spectra.

In addition to the information about the surface structure, the valence band spectra also contain the VBM to surface Fermi level separation. By extrapolating the leading edge of the valence band emission to the base line, the VBM to surface Fermi level separation is found to be 1.32 ± 0.10 eV for all three samples. Although this method is known to slightly underestimate the VBM to surface Fermi level separation in InN,[31] these results confirm, with cleaned samples, the lack of polarity dependence of the surface Fermi level that was suggested by the spectra from the untreated samples. This polarity independence of the Fermi level at InN surfaces contrasts markedly from the 1.4 eV difference between the Fermi levels at the surface of Ga-polarity and N-polarity GaN due to spontaneous polarization.[7,32]

Additionally, the Pt/GaN Schottky barrier height has been found to vary with GaN polarity.[33] The Pt/GaN$(000\bar{1})$ Schottky barrier height is found to be 0.30 eV below the value predicted by the metal induced gap states model taking into account the charge transfer at the interface due to the electronegativity difference between the Pt and the GaN. The deviation from the predicted value for the N-polarity case was explained by including the spontaneous polarization charge in the interface charge balance, resulting in a decrease of the calculated barrier height of 0.33 eV, in very good agreement with the measured value. An *increase* in the barrier height of similar magnitude would also be expected in the Ga-polarity case. However, this was not found in the experiment—the Pt/GaN(0001) Schottky barrier height was found to be very close to the value calculated when no spontaneous polarization charge is included. This initially unexpected behavior was explained by Lüth as being due to the presence of more than two layers of Ga on the surface of Ga-polarity GaN.[33] The metallic character of the interface on the semiconductor side causes considerable screening of the polarization charge, establishing a situation where the internal polarization has negligible effect.[33] The polarization charge still influences the Schottky barrier height at interfaces with N-polarity GaN because it has a surface Ga coverage of only ~1 ML, insufficient to efficiently screen the polarization charge.

The screening of the polarization charge by metallic adlayers, therefore, provides an explanation for the polarity independence of the surface Fermi level and electron accumulation at InN surfaces. In the case of InN, the surfaces of both In- and N-polarity films have at least 2 ML of In at the surface, enough to screen the polarization charge.

IV. CONCLUSION

The surfaces of In- and N-polarity InN have been investigated using core-level and valence band XPS. From the ratio of the In and N core-level XPS signal intensities, the clean In- and N-polarity InN surfaces have been found to be terminated by ~3.4 and ~2.0 ML of In, in each case 1 ML more than for Ga on GaN surfaces grown under Ga-rich conditions. The differing In-adlayer coverages are consistent with the previously observed polarity dependence of InN molecular-beam epitaxy, whereby In-polarity InN can be grown more smoothly than the N-polar material. The valence band XPS indicates a valence band maximum to surface Fermi level separation of 1.32 ± 0.10 eV for both In- and N-polarity InN surfaces, indicating that the surface space charge is independent of polarity as a result of efficient screening of the spontaneous polarization charge by the In adlayers.

ACKNOWLEDGMENTS

We are grateful to Danny Law and Graham Beamson of NCESS for their assistance with the XPS experiments. The Engineering and Physical Sciences Research Council, U.K. is acknowledged for access to the NCESS facility under Grant No. GR/S14252/01 and for financial support under Grant No. EP/C535553/01.

*tim.veal@physics.org

†Present address: Department of Physics, Nanjing University, Nanjing 210093, China.

[1] Hai Lu, W. J. Schaff, L. F. Eastman, and C. E. Stutz, Appl. Phys. Lett. **82**, 1736 (2003).

[2] K. A. Rickert, A. B. Ellis, F. J. Himpsel, Hai Lu, W. Schaff, J. M. Redwing, F. Dwikusuma, and T. F. Kuech, Appl. Phys. Lett. **82**, 3254 (2003).

[3] I. Mahboob, T. D. Veal, C. F. McConville, Hai Lu, and W. J. Schaff, Phys. Rev. Lett. **92**, 036804 (2004).
[4] L. Colakerol, T. D. Veal, H. Jeong, L. Plucinski, A. DeMasi, T. Learmonth, P. Glans, S. Wang, Y. Zhang, L. F. J. Piper, P. H. Jefferson, A. Fedorov, T. Chen, T. D. Moustakas, C. F. McConville, and K. E. Smith, Phys. Rev. Lett. **97**, 237601 (2006).
[5] I. Mahboob, T. D. Veal, L. F. J. Piper, C. F. McConville, H. Lu, W. J. Schaff, J. Furthmüller, and F. Bechstedt, Phys. Rev. B **69**, 201307(R) (2004).
[6] D. Segev and C. G. Van de Walle, Europhys. Lett. **76**, 305 (2006).
[7] H. W. Jang, K. W. Ihm, T.-H. Kang, J.-H. Lee, and J.-L. Lee, Phys. Status Solidi B **240**, 451 (2003).
[8] G. Koblmüller, R. Averbeck, H. Riechert, and P. Pongratz, Phys. Rev. B **69**, 035325 (2004).
[9] J. E. Northrup, J. Neugebauer, R. M. Feenstra, and A. R. Smith, Phys. Rev. B **61**, 9932 (2000).
[10] A. R. Smith, R. M. Feenstra, D. W. Greve, J. Neugebauer, and J. E. Northrup, Phys. Rev. Lett. **79**, 3934 (1997).
[11] T. K. Zywietz, J. Neugebauer, M. Scheffler, and J. E. Northrup, arXiv:physics/9810003 (unpublished).
[12] C. D. Lee, Y. Dong, R. M. Feenstra, J. E. Northrup, and J. Neugebauer, Phys. Rev. B **68**, 205317 (2003).
[13] H. Chen, R. M. Feenstra, J. E. Northrup, T. Zywietz, J. Neugebauer, and D. W. Greve, J. Vac. Sci. Technol. B **18**, 2284 (2000).
[14] D. Segev and C. G. Van de Walle, Surf. Sci. **601**, L15 (2007).
[15] L. F. J. Piper, T. D. Veal, M. Walker, I. Mahboob, C. F. McConville, Hai Lu, and W. J. Schaff, J. Vac. Sci. Technol. A **23**, 617 (2005).
[16] E. Dimakis, E. Iliopoulos, K. Tsagaraki, and A. Georgikilas, Appl. Phys. Lett. **86**, 133104 (2005).
[17] G. Koblmüller, C. S. Gallinat, S. Bernardis, J. S. Speck, G. D. Chern, E. D. Readinger, H. Shen, and M. Wraback, Appl. Phys. Lett. **89**, 071902 (2006).
[18] X. Wang, S.-B. Che, Y. Ishitani, and A. Yoshikawa, Jpn. J. Appl. Phys., Part 2 **45**, L730 (2006).
[19] L. F. J. Piper, T. D. Veal, P. H. Jefferson, C. F. McConville, F. Fuchs, J. Furthmüller, F. Bechstedt, Hai Lu, and W. J. Schaff, Phys. Rev. B **72**, 245319 (2005).
[20] E. S. Hellman, MRS Internet J. Nitride Semicond. Res. **3**, 11 (1998).
[21] D. Muto, T. Araki, H. Naoi, F. Matsuda, and Y. Nanishi, Phys. Status Solidi A **202**, 773 (2005).
[22] Y. Hayakawa, D. Muto, H. Naoi, A. Suzuki, T. Araki, and Y. Nanishi, Jpn. J. Appl. Phys., Part 2 **45**, L384 (2006).
[23] G. R. Bell, N. S. Kaijaks, R. J. Dixon, and C. F. McConville, Surf. Sci. **401**, 125 (1998).
[24] J. Wang, R. So, Y. Liu, H. Wu, M. H. Xie, and S. Y. Tong, Surf. Sci. **600**, L169 (2006).
[25] N. Takeuchi, A. Selloni, T. H. Myers, and A. Doolittle, Phys. Rev. B **72**, 115307 (2005).
[26] S. Tanuma, C. J. Powell, and D. R. Penn, Surf. Interface Anal. **21**, 165 (1994).
[27] U. Grossner, J. Furthmüller, and F. Bechstedt, Appl. Phys. Lett. **74**, 3851 (1999).
[28] J. Neugebauer, Phys. Status Solidi B **227**, 93 (2001).
[29] H. Chen, R. M. Feenstra, J. Northrup, J. Neugebauer, and D. W. Greve, MRS Internet J. Nitride Semicond. Res. **6**, 11 (2001).
[30] R. A. Beach, E. C. Piquette, T. C. McGill, and T. J. Watson, MRS Internet J. Nitride Semicond. Res. **4S1**, G6.26 (1999).
[31] P. D. C. King, T. D. Veal, P. H. Jefferson, C. F. McConville, Hai Lu, and W. J. Schaff, Phys. Rev. B **75**, 115312 (2007).
[32] H. W. Jang, J.-H. Lee, and J.-L. Lee, Appl. Phys. Lett. **80**, 3955 (2002).
[33] H. Lüth, Phys. Status Solidi A **187**, 33 (2001).